Uranyl Incorporation in Natural Calcite

S. D. KELLY,[†] M. G. NEWVILLE,[‡] L. CHENG,[†] K. M. KEMNER,[†] S. R. SUTTON,[‡] P. FENTER,[†] N. C. STURCHIO,*[,†,§] AND C. SPÖTL[||]

Environmental Research Division, Argonne National Laboratory, Argonne, Illinois 60439, Consortium for Advanced Radiation Sources and Department of Geophysical Sciences, University of Chicago, Chicago, Illinois 60637, Department of Earth and Environmental Sciences, University of Illinois at Chicago, Chicago, Illinois 60607-7059, and Institut für Geologie und Paläontologie, Universität Innsbruck, 6020 Innsbruck, Austria

The occurrence of trace amounts of uranyl in natural calcite has posed a long-standing problem in crystal chemistry because of speculation that the size and shape of the uranyl ion may preclude its incorporation in a stable lattice position in calcite. This also defines an important environmental problem because of its bearing on the transport and sequestration of uranyl released from nuclear facilities and uranium mining operations. Calcite is a nearly ubiquitous mineral in soils and groundwater aquifers. X-ray absorption spectroscopy and X-ray fluorescence microprobe studies of uranium in relatively U-rich ~13 700-year-old calcite from a speleothem in northernmost Italy indicate substitution of uranyl for a calcium and two adjacent carbonate ions in calcite. These new data imply that uranyl has a stable lattice position in natural calcite, indicating that it may be reliably sequestered in calcite over long time scales.

Introduction

Uranium (U) is the most common radionuclide contaminant in soils and groundwaters at DOE nuclear facilities and uranium mining operations in the United States. Calcite is nearly ubiquitous in soils and groundwater aquifers and could play an important role in the transport and sequestration of U in the environment. Hexavalent uranium (U^{6+}) in the form of uranyl is the most common species of uranium in soils and surface waters as well as oxic seawater and oxic groundwaters; therefore, uranyl is the form of uranium most likely to be incorporated in calcite precipitated in such waters. The incorporation of the uranyl (UO_2^{2+}) oxo-cation in calcite has been a long-standing problem in geochemistry, however, because the size and shape of the linear uranyl moiety (O═U═O) are significantly different than those of the Ca^{2+} ion for which it may substitute in the calcite structure (*1*). Chemical data from experimental and analytical studies indicate that uranyl behaves as a dilute solid−solution in both aragonite and calcite (*1*−*9*). In contrast, one study concluded that U in planktonic foraminifera is not within the calcite lattice but resides either interstitially or within organic material incorporated within the test (*10*). The solid−liquid distribution coefficients [$(U/Ca_{solid})/(U/Ca_{liquid})$] measured experimentally for uranyl in aragonite and calcite are on the order of ~1−10 and ~0.01−0.1, respectively (*1*−*4*), indicating that the structure of aragonite is more compatible with uranyl substitution than the structure of calcite. Recent X-ray absorption fine structure (XAFS) spectroscopic studies of synthetic, relatively uranyl-rich aragonite and calcite have shown that uranyl coordination in aragonite is similar to that of the uranyl triscarbonato complex $UO_2(CO_3)_3^{4-}$ in aqueous solution (*9*). This indicates that uranyl incorporation from aqueous solution into aragonite requires no change in coordination. Uranyl incorporation into calcite, however, apparently requires change in coordination and may involve local disruption of the calcite structure (*9*). On the basis of spectroscopic studies of uranyl in synthetic calcite, it has been suggested that there may be no stable structural configuration for uranyl in calcite (*8*). The only published high-resolution XAFS measurement for U in a natural calcite to date is that for relatively U-rich calcite (~35 μg/g of U) from a Tennessee ore deposit showing tetravalent U substituting in the Ca position (*11*). Direct structural measurement of U coordination in calcite at natural concentration levels (typically 0.1−10 μg/g of U) is difficult to obtain. New XAFS and X-ray microprobe data were obtained recently for another relatively U-rich (~360 μg/g of U) calcite from a 13 700-year-old speleothem deposit in the Vinschgau Valley of northernmost Italy (*12*). These data, presented here, may be representative of the location of uranyl in typical natural calcites having lower U concentrations.

Experimental Methods

Experimental Setup. The relatively U-rich calcite examined for this study (sample LAS-20) is from a 13 700-year-old speleothem deposit in the Vinschgau Valley of northern Italy (*12*). The sample was prepared in three ways for X-ray measurements at the Advanced Photon Source (APS): as a powder for X-ray diffraction measurements, as a 100-μm-thick doubly polished thin-section for X-ray microprobe measurements, and as a 0.5 × 2 × 3 cm block for XAFS measurements. A bulk U concentration of 362 ± 6 μg/g was measured by isotope dilution α-spectrometry of the powdered sample.

X-ray Diffraction. Powder diffraction measurements performed at APS beamline 12-BM in transmission geometry with monochromatic X-rays (wavelength = 0.6357 Å) indicated that the sample is >99.8% pure calcite.

X-ray Fluorescence Mapping. X-ray microprobe scans were performed at APS beamline 13-ID using a doubly focused, monochromatic X-ray beam from APS undulator A. The X-ray energy was set to 17.3 keV (well above the U L_3 edge) with a double-crystal Si(111) monochromator, adjusting the undulator gap to give maximum intensity at that energy. The X-ray beam was focused to 5 μm × 5 μm using Kirkpatrick-Baez mirrors, which also provided harmonic rejection. The sample was rastered across this beam in 20-μm steps. At each position, fluorescence intensities for Ca K_α, U L_α, and Sr K_α were collected using a 16-element Ge solid-state detector.

X-ray Absorption Spectroscopy. Fluorescence XAFS measurements at the U L_3 absorption edge (17166 eV) were performed at the Materials Research Collaborative Access Team (MR-CAT) (*13*) beamline 10-ID at the APS at Argonne National Laboratory. Incident X-ray energy was selected by using a double-crystal Si(111) monochromator. The undu-

* Corresponding author e-mail: sturchio@uic.edu; telephone: (312)355-1182; fax: (312)413-2279.
[†] Argonne National Laboratory.
[‡] University of Chicago.
[§] University of Illinois at Chicago.
[||] Universität Innsbruck.

10.1021/es025962f CCC: $25.00
Published on Web 00/00/0000

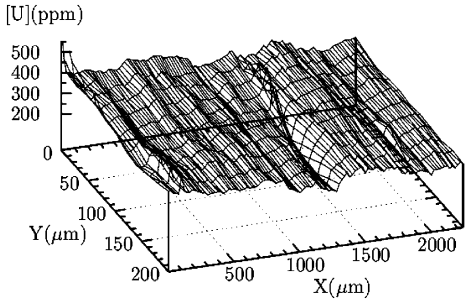

FIGURE 1. X-ray fluorescence map of calcite sample LAS-20 (*12*), showing U concentration as a function of position. The U concentration is normalized to that of Ca to account for changes in thickness of the sample.

lator was tapered to reduce the variation of the incident intensity to less than 15% over the scanned energy range. X-rays of higher harmonic energies were rejected by reflection from a Rh mirror. Incident X-ray intensity was monitored with a N_2-filled ion chamber, and the filtered (3 absorption lengths of Sr) fluorescent X-ray intensity was monitored with an Ar-filled ion chamber in the Stern-Heald geometry (*14*); linearity tests (*15*) indicated less than 0.3% nonlinearity for a 50% decrease in incident X-ray intensity. Ten 2-min XAFS scans were collected at each of six different locations on the sample to minimize possible radiation-induced changes. No time-dependent change in the XAFS data was observed, indicating the absence of detectable radiation damage to the sample.

The UWXAFS package (*16*) was used to analyze the XAFS data. The program FEFF7 (*17*) was used to construct the theoretical model on the basis of the crystallographic atomic positions of andersonite (*18*). The error analysis and the goodness-of-fit parameters were calculated by the fitting routine FEFFIT (*19*). The theoretical models are built from the scattering paths of the photoelectron (created by the absorption of an X-ray) from the first few neighboring shells of atoms about the U atoms in the sample. The structural parameters determined in a fit to the data include the number of atoms in a shell (N_{degen}) about the absorbing atom and the distance (R) to that shell and the mean-square displacement (σ^2) of the distance between the absorbing atom and the neighboring atom for a single scattering path of the photoelectron.

Results and Discussion

X-ray Fluorescence Mapping. Results from the X-ray fluorescence (XRF) mapping indicate that the U concentration in a portion of the calcite varies from about 80 to 500 ppm and is fairly homogeneous at the 100-μm scale (Figure 1). There is no evidence for U-rich inclusions at the scale of the beam spot size (5 μm). These XRF data are consistent with the occurrence of U in a dilute solid−solution within the calcite.

X-ray Absorption Spectroscopy. The X-ray absorption spectra of the calcite sample and the uranyl nitrate hexahydrate [$UO_2(NO_3)_2$·$6H_2O$] reference compound have indistinguishable peak edge energies at 17167 eV (Figure 2), indicating that U in the sample is dominantly hexavalent.

The XAFS data and best-fit model are shown in Figure 3. The presence of peaks between 1 and 4 Å in the magnitude of the Fourier transform (FT) of the XAFS data show that U occupies a regular and well-defined crystallographic site in the calcite sample (Figure 4). The two largest peaks in the magnitude of the FT (appearing at 1.0−2.2 Å in the FT) correspond to the two axial oxygen (O_{ax}) and approximately four (3.8 ± 0.4) equatorial oxygen (O_{eq}) atoms of the uranyl, with a U−O_{ax} distance of 1.80 ± 0.01 Å and a U−O_{eq} distance

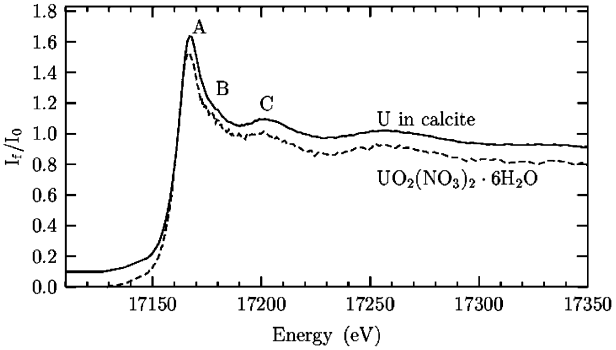

FIGURE 2. Normalized X-ray absorbance for U L_{III} edge showing XAFS for U in calcite sample LAS-20 (solid) and for uranyl nitrate hexahydrate reference compound (dashed). The similarities in energy and intensity of features A (white line at 17167 eV), B (shoulder at 17178 eV), and C (at 17202 eV) indicate that U is present as UO_2^{2+} in calcite.

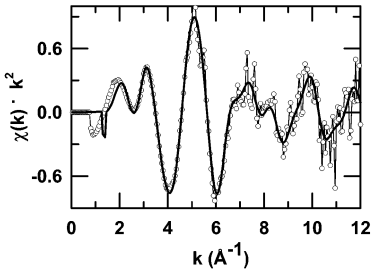

FIGURE 3. XAFS $\chi(k)k^2$ data (open circles) and best-fit model (thick line) for calcite LAS-20.

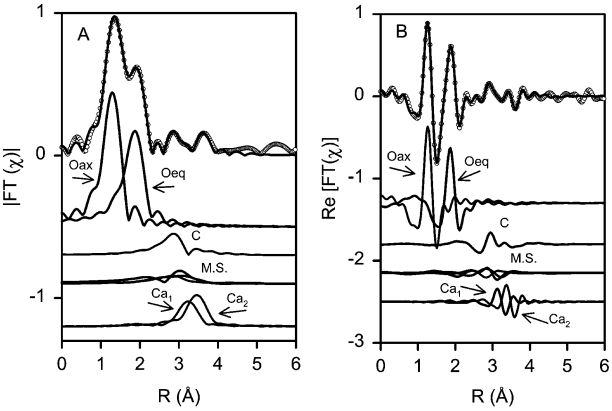

FIGURE 4. XAFS data (open circles) and best-fit model (thick line) are shown at the top of each figure for calcite LAS-20. The magnitude (A) and real part (B) of the Fourier transform of $\chi(k)k^2$ are shown separately. Under the data and best-fit model, the individual contributions to the model for each scattering path are shown. The data were processed by using $\Delta k = 2.0-10.5$ Å^{-1} and $\Delta R = 1.1-3.9$ Å. A Hanning window was used in the Fourier transform with a full sill width of 1.0 Å^{-1}. The data and Fourier transform ranges resulted in 17 degrees of freedom and 3 independent points in the fit.

of 2.41 ± 0.01 Å, respectively. Beyond these two shells, there is a signal from a shell (appearing at 2.2−3.2 Å in the FT) containing approximately four (4.3 ± 2.7) C atoms with a U−C distance of 3.51 ± 0.04 Å. Next, there is a signal from a split Ca shell. Our best-fit model for the XAFS data has the six Ca atoms found in calcite split into two shells with approximately two (2.3±0.4) calcium (Ca_1) atoms with a U−Ca_1 distance of 3.78 ± 0.03 Å and approximately four (3.7±0.4) calcium (Ca_2) atoms with a U−Ca_2 distance of 4.01±0.02 Å.

TABLE 1. EXAFS Model Parameters for the Calcite Sample LAS-20 (*12*)

path	R^a	N_{degen}	ΔR (Å)	σ^2 (Å^2)	ΔE_0 (eV)^c
		U−Calcite			
U−O_{ax}	1.78	2^b	ΔR_1	σ^2_1	ΔE_1
U−O_{eq}	2.41	N_1	ΔR_2	σ^2_1	ΔE_2
U−C	3.69	N_3	ΔR_4	σ^2_3	ΔE_2
U−O_{ax1}−O_{ax2}	3.55	2^b	$2\Delta R_1$	$2\sigma^2_1$	ΔE_1
U−O_{ax1}−U−O_{ax1}	3.58	2^b	$2\Delta R_1$	$2\sigma^2_1$	ΔE_1
U−O_{ax1}−U−O_{ax2}	3.58	2^b	$2\Delta R_1$	$2\sigma^2_1$	ΔE_1
U−Ca_1	3.96	N_4	ΔR_5	σ^2_4	ΔE_2
U−Ca_2	3.96	6 − N_4	ΔR_6	σ^2_4	ΔE_2

^{a} The initial path length. ^{b} These values were not varied in the fit. ^{c} Energy shift of the photoelectron.

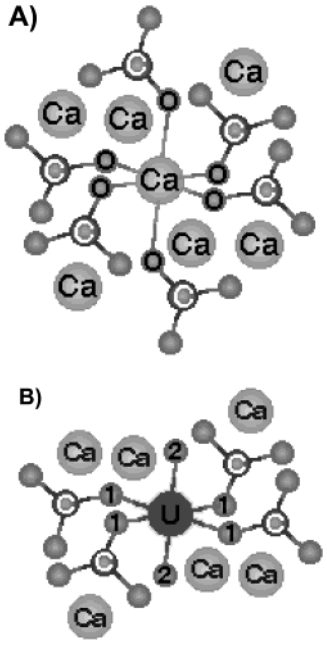

FIGURE 5. (A) Diagram showing calcite structure about a Ca^{2+} ion. (B) Diagram showing the local structure of uranyl incorporated into calcite that is consistent with the XAFS data. The numerals 1 and 2 indicate O_{eq} and O_{ax} atoms, respectively.

The model described above (Table 1) and shown in Figures 3 and 4 is in good agreement with the XAFS data and is consistent with the uranyl ion substituting for one Ca and two carbonate ions in the calcite structure. Calcium in calcite (Figure 5A) is coordinated by six O atoms at 2.36 Å. Each of these O atoms is a part of a carbonate group with a C atom at 3.21 Å, and there are six neighboring Ca atoms at 4.05 Å. According to our model (Figure 5B), uranium in calcite is also coordinated by six O atoms, two of which are the O_{ax} atoms of the uranyl leaving four (3.8 ± 0.4) O_{eq} atoms that are each a part of a carbonate group with four (4.3 ± 2.7) C atoms at 3.51 ± 0.04 Å and there are a total of six Ca atoms at 3.78−4.01 Å from the U atom.

The distances to the neighboring shells and their mean-square displacement values of atoms determined for U in calcite (Table 2) are similar to those found for Ca in calcite and also to those found in other uranyl coordination environments. The best-fit values for the U−O_{ax} shell distance (1.80 ± 0.01 Å) and mean-square displacement (0.002 ± 0.001 Å^2) in the calcite sample are consistent with other reported values for the U−O_{ax} distance (R = 1.78−1.81 Å) and σ^2 (0.001−0.004 Å^2) (*8*, *9*, *20*−*22*). The best-fit value for the U−O_{eq} shell mean-square displacement (0.006 ± 0.002 Å^2) is also consistent with other reported values (0.003-0.010 Å^2) (*8*, *9*, *20*−*22*). The best-fit value U−O_{eq} distance in the sample (2.41 ± 0.01 Å) is comparable to that for uranyl having 6 equatorial oxygens (2.43 Å) (*23*), such as for the uranyl triscarbonato aqueous complex, which has three carbonate ions bonded in bidentate fashion symmetrically about the uranyl equatorial plane. Despite this similarity in U−O_{eq} bond length, the best-fit value for the number of equatorial oxygens about uranyl in the sample is 3.8 ± 0.4, which is consistent with bonding of four carbonates in monodentate fashion about the uranyl equatorial plane. Furthermore, the best-fit value for the U−C distance in the sample (3.51 ± 0.04 Å) is much larger than the typical U−C distance for carbonates with bidentate bonding to uranyl (2.9 Å) (*23*) but more similar to the Ca−C distance in calcite (3.21 Å) in which all carbonates have monodentate bonding to Ca. Attempts to model our U XAFS data with bidentate bonding of carbonates to U resulted in significantly poorer qualities of fit, leading us to prefer the model in which uranyl substitutes for Ca with local relaxation of carbonates.

TABLE 2. Best-Fit Values for XAFS Model of Calcite Sample LAS-20 (*12*)^a

path	N_{degen}	R (Å)	σ^2 (10^{-3} Å^2)	ΔE_0 (eV)
		U−Calcite		
U−O_{ax}	2	1.80 ± 0.01	2 ± 1	6.1 ± 1.5
U−O_{eq}	3.8 ± 0.4	2.41 ± 0.01	6 ± 2	7.8 ± 1.0
U−C	4.3 ± 2.7	3.51 ± 0.04	7 ± 11	7.8 ± 1.0
U−O_{ax1}−O_{ax2}	2	3.61 ± 0.02	5 ± 1	6.1 ± 1.5
U−O_{ax1}−U−O_{ax1}	2	3.61 ± 0.02	5 ± 1	6.1 ± 1.5
U−O_{ax1}−U−O_{ax2}	2	3.61 ± 0.02	5 ± 1	6.1 ± 1.5
U−Ca_1	2.3 ± 0.4	3.78 ± 0.03	7 ± 4	7.8 ± 1.0
U−Ca_2	3.7 ± 0.4	4.01 ± 0.02	7 ± 4	7.8 ± 1.0

^{a} Values without uncertainties were constrained to the value listed.

The proposed substitution results in net charge excess around the uranyl site of +4 because of the two missing carbonate ions. This charge excess could be compensated by a coupled, nonlocal substitution such as $5Ca^{2+} \Rightarrow UO_2^{2+} + 4Na^+$, which is consistent with our XAFS data and the elevated concentration of sodium (337 μg/g) in this calcite (*12*). The absence of the carbonate ions must create a significant defect in the local calcite structure; however, it is not clear how this might be accommodated. Substitution of water or hydroxyl for the missing carbonate may be possible. The U XAFS data do not allow determination of the exact substitution formula. The split U−Ca shell (approximately two Ca_1 atoms at a shorter distance of 3.78 Å and approximately four Ca_2 atoms at 4.01 Å) is not surprising. The two Ca_1 atoms are most likely those nearest in the adjacent (104) planes that relax toward the uranyl position (Figure 5B) because of the displaced carbonate groups. The remaining four Ca_2 atoms are at about the same distance from U (4.01 Å) as the Ca−Ca distance in calcite (4.05 Å).

Summary

Our XAFS results for the incorporation of uranyl into natural calcite differ significantly from those reported recently for uranyl-rich synthetic calcite (*8*, *9*). The synthetic calcite has an O_{eq} coordination number of five, suggesting two bidentate linkages and one monodentate linkage with carbonate ions in the equatorial plane (*8*, *9*). However, our best-fit results for the natural calcite indicate four monodentate linkages with carbonate ions in the equatorial plane, which is essentially the same coordination as Ca in calcite (Figure 5A,B). The total first-shell O coordination of the U^{6+} in our natural calcite sample is 6-fold, the same as Ca in calcite, rather than 7-fold as reported for U^{6+} in synthetic calcite (*8*, *9*). No U−Ca backscatter was detected in the synthetic calcite, indicating either multiple or disordered sites for uranyl (*8*,

9). This is not the case for the natural sample that we examined, however, where six Ca atoms occur in a split shell having an average U−Ca distance (3.93 Å) similar to that of the Ca−Ca distance in calcite (4.05 Å). The splitting of the O and Ca shells and the 4-fold coordination of the U−C shell are consistent with our model of substitution of uranyl for Ca in calcite, with U^{6+} substituting for Ca and O_{ax} substituting for the nearest carbonate ions in the adjacent (104) layers (see Figure 5).

The excellent agreement between the best-fit model and the XAFS data indicates that uranyl occupies a relatively stable position in this calcite. Uranyl in rapidly grown, synthetic, uranyl-rich calcite (*8*, *9*) is apparently more likely to reside in defects or other, more disordered sites than that identified here. Our results for this 13 700-year-old natural calcite indicate either that natural calcite grows slowly enough to allow for ordering of incorporated uranyl during growth or that structural transformation of initially disordered uranyl in calcite may occur over a long time (*8*). Petrographic evidence indicates that this calcite formed by recrystallization of uranium-rich aragonite (*12*), for which our XAFS measurements also showed U^{6+}. This mechanism of formation (in a closed system) could explain the relatively high uranyl concentration by inheritance from the aragonite. The relatively high uranyl concentration of the precursor aragonite reflects its precipitation from uranium-rich groundwater circulating through crystalline basement rocks (*12*).

The stable position of uranyl in relatively uranyl-rich natural calcite, identified by analysis of our XAFS data, may provide a resolution to the problem of the location of trace uranyl in calcite. Further XAFS studies of uranyl-bearing natural calcite from a variety of contrasting geochemical environments are recommended to test the general applicability of this result. If the position of uranyl in natural calcite is generally as described above, calcite may provide a stable host for dispersed U^{6+} over geological time scales, which is a result that has important bearing on the environmental fate and transport of aqueous uranyl.

Acknowledgments

This work was supported by the U.S. Department of Energy, Offices of Basic Energy Sciences (Geosciences Research Program) and Biological and Environmental Research (NABIR Program). We thank E. J. O'Loughlin and J. H. Terry for assistance with XAFS measurements and R. J. Reeder and two anonymous reviewers for helpful reviews of the manuscript. The Advanced Photon Source is supported by the U.S. Department of Energy, Office of Science, Office of Basic Energy Sciences. Work performed at MRCAT (beamline 10-ID) is supported, in part, by funding from the Department of Energy (Grant DEFG0200ER45811). This work was created by the University of Chicago as operator of Argonne National Laboratory under Contract W-31-109-ENG-38 with the U.S. Department of Energy.

Literature Cited

(1) Russell, A. D.; Emerson, S.; Nelson, B. K.; Erez, J.; Lea, D. W. *Geochim. Cosmochim. Acta* **1994**, *58*, 671.
(2) Kitano, Y.; Oomori, T. *J. Ocean Sci. Jpn.* **1971**, *27*, 34−42.
(3) Carroll, S.; Bruno, J. *Radiochim. Acta* **1991**, *52*−*53*, 187−193.
(4) Meece, D. E.; Benninger, J. K. *Geochim. Cosmochim. Acta* **1993**, *57*, 1447−1458.
(5) Shen, G. T.; Dunbar, R. B. *Geochim. Cosmochim. Acta* **1995**, *59*, 2009−2024.
(6) Min, G. R.; Edwards, R. L.; Taylor, F. W.; Recy, J.; Gallup, C. D.; Beck, J. W. *Geochim. Cosmochim. Acta* **1995**, *59*, 2025−2042.
(7) Geipel, G.; Reich, T.; Brendler, V.; Bernhard, G.; Nitsche, H. *J. Nucl. Mater.* **1997**, *248*, 408−411.
(8) Reeder, R. J.; Nugent, M.; Drew Tait, C.; Morris, D. E.; Heald, S. M.; Beck, K. M.; Hess, W. P.; Lanzirotti, A. *Geochim. Cosmochim. Acta* **2001**, *65*, 3491−3503.
(9) Reeder, R. J.; Nugent, M.; Lamble, G. M.; Tait, C. D.; Morris, D. E. *Environ. Sci. Technol.* **2000**, *34*, 638−644.
(10) Henderson, G. M.; O'Nions, R. K. *Geochim. Cosmochim. Acta* **1994**, *59*, 4685−4694.
(11) Sturchio, N. C.; Antonio, M. R.; Soderholm, L. B.; Sutton, S. R.; Brannon, J. C. *Science* **1998**, *281*, 971−973.
(12) Spötl, C.; Unterwurzacher, M.; Mangini, A.; Longstaffe, F. J. *J. Sediment. Res.* **2002**, *72*, 793−808.
(13) Segre, C. U.; Leyarovska, N. E.; Chapman, L. D.; Lavender, W. M.; Plag, P. W.; King, A. S.; Kropf, A. J.; Bunker, B. A.; Kemner, K. M.; Dutta, P.; Druan, R. S.; Kaduk, J. *Synchrotron Radiation Instrumentation*; Eleventh U.S. Conference; CP521; 2000; pp 419−422.
(14) Stern, E. A.; Heald, S. M. *Rev. Sci. Instrum.* **1979**, *50*, 1579−1583.
(15) Kemner, K. M.; Kropf, A. J.; Bunker, B. A. *Rev. Sci. Instrum.* **1994**, *65*, 3667−3669.
(16) Stern, E. A.; Newville, M.; Ravel, B.; Yacoby, Y.; Haskel, D. *Physica B* **1995**, *208/209*, 2995−3009.
(17) Zabinsky, S. I.; Rehr, J. J.; Ankudinov, A.; Albers, R. C.; Eller, M. J. *Phys. Rev. B* **1995**, *52*, 2995−3009.
(18) Coda, A.; Della Giusta, A.; Tazzoli, V. *Acta Crystallogr.* **1981**, *B37*, 1496−1500.
(19) Newville, M.; Ravel, B.; Haskel, D.; Stern, E. A. *Physica B* **1995**, *208/209*, 154−156.
(20) Bargar, J. R.; Reitmeyer, R.; Lenhart, J. J.; Davis, J. A. *Geochim. Cosmochim. Acta* **2000**, *64*, 2737−2749.
(21) Allen, P. G.; Shuh, D. K.; Bucher, J. J.; Edelstein, N. M.; Reich, T.; Denecke, M. A.; Nitsche, H. *Inorg. Chem.* **1996**, *35*, 784−787.
(22) Allen, P. G.; Bucher, J. J.; Clark, D. L.; Edelstein, N. M.; Ekberg, S. A.; Gohdes, J. W.; Hudson, E. A.; Kaltsoyannis, N.; Lukens, W. W.; Neu, M. P.; Palmer, P. D.; Reich, T.; Shuh, D. K.; Tait, C. D.; Zwick, B. D. *Inorg. Chem.* **1995**, *34*, 4797−4807.
(23) Burns, P. C. *Uranium: Mineralogy, Geochemistry and the Environment*; Mineralogical Society of America: Washington, DC, 1999.

Received for review July 11, 2002. Revised manuscript received January 2, 2003. Accepted January 13, 2003.

ES025962F